

## INFLUENCE OF ARSENIC, ANTIMONY AND BISMUTH ON THE PROPERTIES OF LEAD/ACID BATTERY POSITIVE PLATES

D. PAVLOV\*, A. DAKHOUCHE and T. ROGACHEV

Central Laboratory of Electrochemical Power Sources, Bulgarian Academy of Sciences, Sofia 1113 (Bulgaria)

---

### Introduction

The positive plates of the lead/acid battery comprise three structural elements: grid, corrosion layer, and active mass. The corrosion layer is formed during battery operation due to the thermodynamic instability of the grid at the positive-plate potentials. During charge and discharge, the electric current flows consecutively through these elements. Since electrochemical processes occur in both the active mass and the corrosion layer, each of these components could become a capacity-limiting parameter.

The reaction area over which the electrochemical processes take place in an automotive battery plate with 100 g active mass is between 400 and 700 m<sup>2</sup>. The area of the corresponding grid is ~100 cm<sup>2</sup>. Evidently, during charge and discharge, the density of the electron flow through the corrosion layer increases considerably. Therefore, the corrosion layer appears to be the most sensitive and critical component of the positive-plate structure.

During discharge of the positive plate, 30 - 50% of the active mass is converted to PbSO<sub>4</sub>. This results in a partial destruction of the PbO<sub>2</sub> skeleton of the active mass, which at charge is restored again. Since these processes are not always reversible, the structure of the active mass gradually disintegrates and the capacity decreases.

The grid of the positive plate is made of lead alloy, most often containing antimony, arsenic, tin, or other alloying additives. Due to the anodic oxidation of the alloy, these additives become incorporated in both the corrosion layer and the active mass, thus playing the role of dopants there. It has been established that such elements exert a considerable effect on the performance of the plate (*e.g.*, 'antimony-free' effect, 'tin-free effect', etc.).

Since antimony has a wide application in the battery industry, its effect on the positive plate has been studied extensively [1 - 15]. Rand *et al.* [3] and Arifuku *et al.* [2] determined the antimony distribution in the corrosion layer. Rogachev *et al.* [12] established the influence of antimony on the corrosion rate for different operation modes of the lead/acid battery. Sweets [6] found a similarity between the crystal structures of  $\alpha$ -PbO<sub>2</sub> and PbSb<sub>2</sub>O<sub>6</sub>. Ritchie

---

\*Author to whom correspondence should be addressed.

and Burbank [8] demonstrated that antimony slows down the volume growth of the  $\text{PbO}_2$  agglomerates and suppresses their crystallinity. Dawson *et al.* [9] discovered that considerably more antimony was adsorbed on the surface of  $\text{PbO}_2$  crystals than on  $\text{PbSO}_4$  crystals. Further,  $\text{Sb}^{5+}$  ions are adsorbed much more easily than  $\text{Sb}^{3+}$  ions. Abdul Azim and Ismail [11] studied the influence of  $\text{Sb}_2\text{O}_3$  and  $\text{As}_2\text{O}_3$  on the cycle life of positive plates. Maja *et al.* [16] established that the presence of antimony as a dopant in the  $\text{PbO}_2$  crystal lattice increases the electrode capacity, whereas when introduced into the solution it has a passivating effect. Yeo and Johnson [17] found that the presence of Group V dopants (bismuth and arsenic) in the  $\text{PbO}_2$  phase accelerates many reactions with oxygen transition.

The aim of the present work is to study the effect of arsenic, antimony and bismuth (Group V metals) on the processes involved in the building up of the structure of the  $\text{PbO}_2$  active mass of lead/acid battery positive plates.

## Experimental

### Procedure

The active mass of automotive battery plates was used in the investigations. The charged active mass was removed from the Pb grids and ground into powder. Tubular electrodes were filled with the  $\text{PbO}_2$  powder and then subjected to charge/discharge cycling.

The dependence of the specific capacity,  $\gamma_c$  (*i.e.*, capacity of 1 g of active material) on the number of cycles was determined. A study was conducted of the influence of arsenic, antimony and bismuth on the rebuilding processes of the active-mass structure and its interaction with the corrosion layer during cycling. The dopants were added either to the grid spine alloy or to the solution.

### $\text{PbO}_2$ powder preparation

Positive and negative plates were produced with pure lead grids and pastes were prepared from a 4.5%  $\text{H}_2\text{SO}_4/\text{PbO}$  mixture at 30 - 50 °C. Plate formation was carried out in  $\text{H}_2\text{SO}_4$  of sp. gr. 1.05. Cells with 50% utilization of the positive active mass were assembled and subjected to 5 charge/discharge cycles at 100% depth-of-discharge (DOD). The active mass was taken off the grids, washed with water, dried at 40 °C for 1 h, and ground to powder. Tubular electrodes were filled with the powder.

### Tubular powder electrode

The design of the tubular powder electrode [18, 19] is schematically presented in Fig. 1. The polyester-fabric tube was filled with  $\text{PbO}_2$  powder of a known weight. A threaded electrode spine was used with plugs at either end that served to contain the powder within a given volume of the tube. It was thus possible to control precisely the density of the powder in the tubular electrode. The height of the spine in contact with the  $\text{PbO}_2$  powder

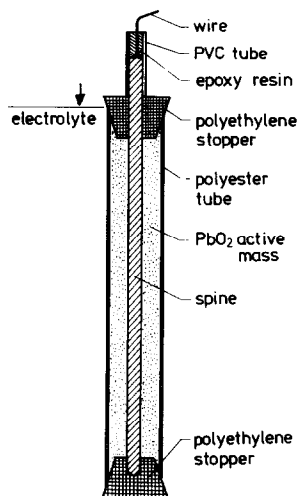


Fig. 1. Schematic of tubular electrode.

(limited by the two plugs) was 52 mm. The spine had a diameter of 4.0 mm and the diameter of the tubular electrode was 9.0 mm.

### Cell design

The cell, consisting of the tubular electrode, two negative plates with lead grids, and an  $\text{Hg}/\text{Hg}_2\text{SO}_4$  reference electrode, was assembled in a glass container. Sulphuric acid solution of sp. gr. 1.28 was used. The cell was left on open circuit for 30 min to allow the tubular electrode to soak up the solution. A charge at  $15 \text{ mA cm}^{-2}$  was carried out for 45 min in order to form a corrosion layer on the surface of the spine. This was followed by a period of 10 min at open circuit, and a discharge at  $15 \text{ mA cm}^{-2}$  to 0 mV *versus* the  $\text{Hg}/\text{Hg}_2\text{SO}_4$  electrode.

## Results and discussion

### *Influence of active-mass density*

Tubular electrodes were prepared with various  $\text{PbO}_2$  powder masses of density ( $d$ ) between  $3.40$  and  $4.50 \text{ g cm}^{-3}$ . The electrodes were subjected to cycling: discharge at  $15 \text{ mA cm}^{-2}$  to cut-off potential of 0 mV, and charge up to a capacity over 200% of the preceding discharge capacity. Figure 2 presents the capacity/cycle number dependence for electrodes with lead spines. The value of the capacity calculated at 50% utilization of the active mass ( $\eta_{\text{st}}$ ) is given for comparison.

There is a critical value of the  $\text{PbO}_2$  powder density above which restoration of the active mass commences. For a pure lead electrode, this critical density is slightly less than  $3.80 \text{ g cm}^{-3}$ . The influence of dopants was

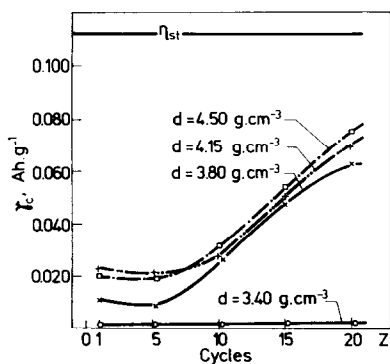


Fig. 2. Dependence of specific capacity of tubular electrodes with different  $\text{PbO}_2$  powder density on cycle life.

studied using electrodes with densities higher than the critical value, namely, 4.15 and  $3.80 \text{ g cm}^{-3}$ . Figure 2 shows that the difference between the capacity curves at  $d = 4.15$  and  $4.50 \text{ g cm}^{-3}$  is very small. Thus, at  $d = 4.15 \text{ g cm}^{-3}$ , the complete capability of the  $\text{PbO}_2$  particles to interconnect into an active-mass skeleton is reached.

After cycling, the polyester tube was cut open. The active mass of the electrodes with a density of  $3.40 \text{ g cm}^{-3}$  had disintegrated into a powder. The electrode structure with a powder density of  $3.80 \text{ g cm}^{-3}$  also disintegrates easily. On the other hand, the mass had preserved its cylindrical shape in electrodes with densities of 4.15 and  $4.50 \text{ g cm}^{-3}$ . During cycling of these electrodes, the skeleton structure of the active mass had been formed.

#### *Influence of arsenic, antimony and bismuth ions in the solution on rebuilding the active-mass structure*

Spines made of pure lead and Pb-6%wt.%Sb alloy were used. The powder electrode density was  $4.15 \text{ g cm}^{-3}$ . The ion concentration in the solution was 0.015 M for  $\text{As}^{3+}$ , 0.0011 M for  $\text{Sb}^{3+}$ , and 0.005 M for  $\text{Bi}^{3+}$  ions. These concentrations were maintained approximately constant during the experiments. Figure 3 shows the resulting capacity curves.

The following conclusions can be drawn from these results.

(i) Comparison of the capacity curves of electrodes cycled in pure  $\text{H}_2\text{SO}_4$  and in doped electrolyte shows that arsenic hinders capacity growth during cycling. Antimony ions also slow down this process; a passivating effect on the discharge processes by antimony ions in the solution was observed by Maja and co-workers [16]. Bismuth ions accelerate and facilitate the development of the active-mass structure. This influence is registered by electrodes with each kind of spine.

(ii) Comparison of Fig. 3(a) and (b) clearly shows that for the first 10 cycles the presence of antimony in the spine assists the capacity development of tubular electrodes.

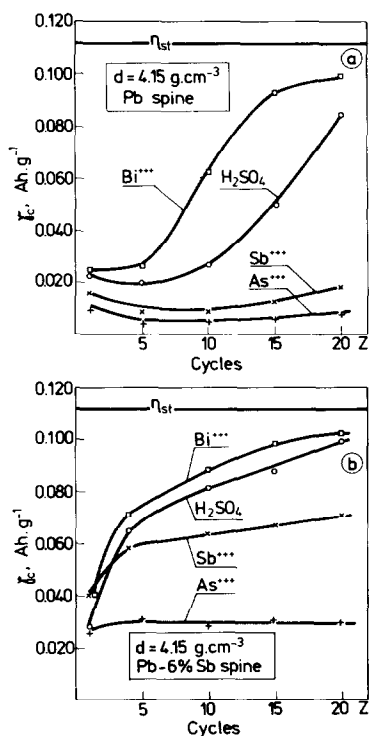


Fig. 3. Influence of arsenic, antimony, and bismuth ions in the solution on specific capacity/cycle life. Tubular electrodes made with (a) lead, (b) Pb-6wt.%Sb spines.

#### *Influence of arsenic in the alloy on restoration of the active-mass structure*

A study was made of the performance of electrodes with spines made from Pb-As alloys of varying arsenic content. Figure 4 presents the capacity as a function of arsenic content and cycle number.

From these data, the following conclusions can be drawn.

(i) Increasing the density of the  $\text{PbO}_2$  powder from  $3.80$  to  $4.15 \text{ g cm}^{-3}$  results in a significant restoration of the active-mass structure. For example, after 20 cycles ( $d = 4.15 \text{ g cm}^{-3}$ ) the capacity reaches values very close to that for an electrode with a 50% active-mass utilization ( $\eta_{st}$ ). The structure restoration is slow and incomplete for a powder density of  $3.80 \text{ g cm}^{-3}$ . Thus, the restoration processes of the active-mass structure are very sensitive to the density when the spine alloy contains As.

(ii) Comparison of the capacity values of electrodes with spines made of pure lead and Pb-As alloys shows that arsenic has an advantageous influence on the restoration processes of the active-material structure: especially for electrodes with the higher active-mass density. For example, the capacity curve for the first cycle of an electrode with an active-mass density of  $4.15 \text{ g cm}^{-3}$  shows that even 0.05 wt.% As in the alloy leads to an almost

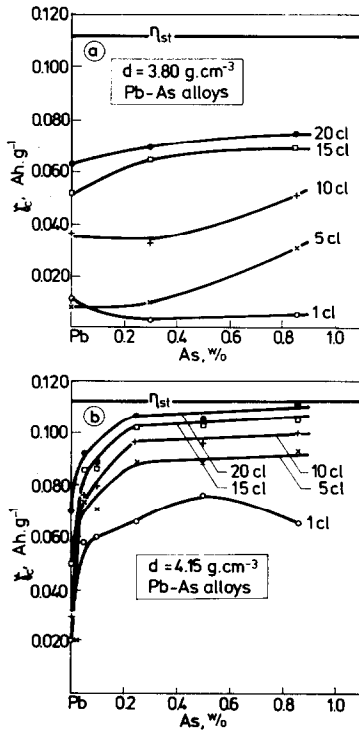


Fig. 4. Influence of arsenic (alloy) concentration on capacity.  $\text{PbO}_2$  powder density: (a)  $4.15 \text{ g cm}^{-3}$ ; (b)  $3.80 \text{ g cm}^{-3}$ . cl = cycle number.

three-fold increase in capacity. When the active-mass density is close to the critical value ( $d = 3.80 \text{ g cm}^{-3}$ ), however, the influence of arsenic is not observed. Indeed, a decrease in capacity occurs. An increase in the arsenic concentration of the alloy from 0.2 to 0.8 wt.% has only a slight influence on the electrode capacity after 20 cycles. The influence of arsenic on the corrosion rate has already been reported [20].

#### *Influence of bismuth in the alloy on restoration of the active-mass structure*

The investigations carried out were analogous to those reported above for Pb-As alloys. The results are presented in Fig. 5. Electrodes with a density of  $4.15 \text{ g cm}^{-3}$  and with differing bismuth contents in the spine alloy were used. It can be seen that the influence of bismuth is very similar to that of arsenic. On the first discharge cycle, the electrodes with Pb-Bi spines and with an active-mass density of  $4.15 \text{ g cm}^{-3}$  exhibit a capacity that is 2.5-3 times greater than that of electrodes with pure lead spines. After 20 cycles, the structure of the active mass is restored to such a degree that the capacity reaches the value for 50% active-mass utilization. This effect appears when the alloy contains more than 0.2 wt.% Bi. The data in Fig. 5 also show that the capacities of the electrodes with both powder densities and Pb-0.8wt.%Bi

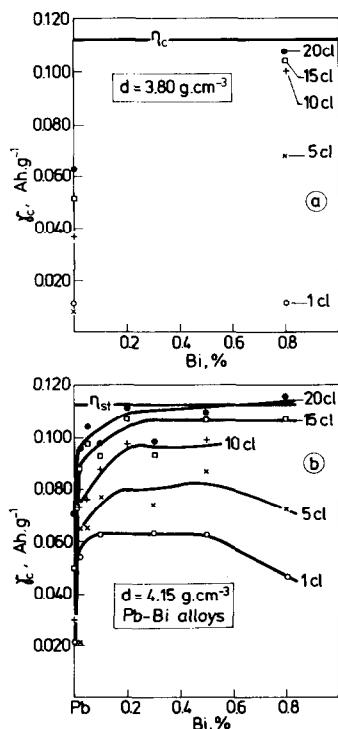


Fig. 5. Influence of bismuth (alloy) concentration on capacity.  $\text{PbO}_2$  powder density: (a)  $4.15 \text{ g cm}^{-3}$ ; (b)  $3.80 \text{ g cm}^{-3}$ . cl = cycle number.

spines are similar. Hence, adding bismuth to the spine alloy renders the electrode less sensitive to the active-mass density.

It was observed that bismuth caused a marked increase in the spine corrosion rate at the spine-electrolyte-air boundary. It is known [17] that when the  $\text{PbO}_2$  layer is doped with bismuth ions there is an acceleration in the transfer of oxygen through the layer. This is the cause of bismuth increasing the corrosion rate. Therefore, the beneficial action of bismuth on the active-mass structure restoration processes is diminished by the effect of bismuth on the spine corrosion layer.

#### *Influence of antimony in the alloy on active-mass structure restoration*

Figure 6 presents the results obtained from investigations of powder tubular electrodes with Pb-Sb spines where antimony is in concentrations used in the battery industry. The influence of antimony is very similar to that of arsenic and bismuth.

At the 20th cycle, the capacity of electrodes with an active-mass powder density of  $3.80 \text{ g cm}^{-3}$  and spines made of 6 and 9 wt.% Sb alloys is equivalent to 50% active-mass utilization. This performance is better than

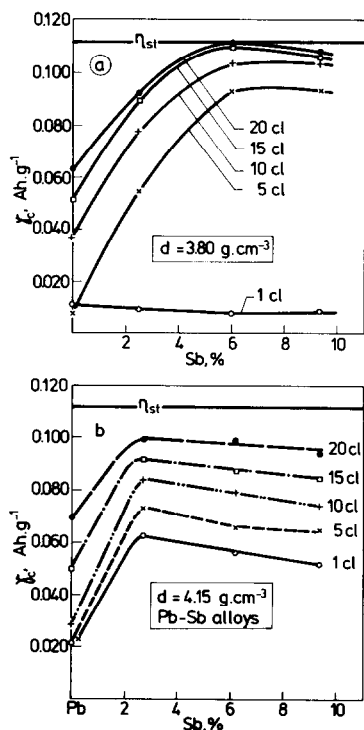


Fig. 6. Influence of antimony (alloy) concentration on capacity. PbO<sub>2</sub> powder density: (a) 4.15 g cm<sup>-3</sup>; (b) 3.80 g cm<sup>-3</sup>. cl = cycle number.

that of electrodes with a powder density of 4.15 g cm<sup>-3</sup>. It is concluded, therefore, that antimony decreases the critical value for the density. During cycling, the active mass is pulsing and its density decreases continuously [21]. The presence of antimony in the alloy provides the electrode with the capability to restore the active-mass structure over a wider range of density. This feature of antimony may be one of the components of the 'antimony-free effect'.

From a comparison of the capacity values at the 20th cycle for electrodes with pure lead and Pb-Sb spines, it is seen that antimony increases the electrode capacity. This effect is especially strong for electrodes with  $d = 3.80 \text{ g cm}^{-3}$ . At this density, the electrode capacity increases very rapidly with cycling. The greater the antimony concentration in the alloy, the higher the capacity growth rate. This shows that antimony influences the kinetics of the active-mass structure restoration.

## Discussion

The experimental results show that, in the case of tubular PbO<sub>2</sub> powder electrodes, a PbO<sub>2</sub> active-mass structure can be evolved during cycling. Its



specific capacity can reach values equal to those obtained for pasted electrodes produced under industrial conditions. The data further indicate that the specific capacity of the tubular powder electrode,  $\gamma_c$ , is a function of the parameters:

$$\gamma_c = f(d, z, CL, D_1, D_2, \dots) \quad (1)$$

where  $d$  is the density of the powder (active mass);  $z$  is the cycle number; CL denotes the corrosion layer (the layer influences the capacity through its conductivity, electrochemical properties and phase composition);  $D_1$  and  $D_2$  represent the effect of additives to the alloy and/or to the electrolyte, respectively.

Through which parts of the electrode is the capacity influenced by the dopants? A model of the tubular powder electrode is presented in Fig. 7. Here, M denotes the spine and AM the active mass. The active mass has the following structure [21, 22]: its smallest building element is the  $PbO_2$  particle (P); many particles are interconnected to form a microporous  $PbO_2$  agglomerate (Agg). The agglomerates, in turn, interconnect to produce a macroporous skeleton. During grinding of the active mass, the skeleton is broken down into separate agglomerates and particles ( $PbO_2$  powder). The tubular electrodes were filled with such powder.

The specific capacity  $\gamma_c$ , can be expressed as:

$$\gamma_c = It_h/g \quad (2)$$

where  $I$  is the discharge current;  $g$  is the active-mass weight;  $t_h$  is the discharge time until the electrode potential reaches 0 mV *versus* Hg/Hg<sub>2</sub>SO<sub>4</sub>;  $t_h$  is a function of the electrode polarization ( $\Delta\phi_P$ ). The latter is equal to the sum of the polarizations at the separate electrode elements and the contacts between them, the polarization of the electrochemical reaction ( $\Delta\phi_{ER}$ ), and the polarization due to ionic transport in the pores of the electrode ( $\Delta\phi_{EI}$ ).

$$\Delta\phi_P = \Delta\phi_{M/CL} + \Delta\phi_{CL} + \Delta\phi_{CL/AM} + \Delta\phi_{Agg} + \Delta\phi_{Pi} + \Delta\phi_{ER} + \Delta\phi_{EI} \quad (3)$$

$\Delta\phi_{Agg}$  represents the polarization at the interface between the  $PbO_2$  powder particles, or agglomerates, from the skeleton of the active mass.  $\Delta\phi_{Pi}$  is the polarization at the interface between  $PbO_2$  particles included in the agglomerates.

The capacity curves for the first and fifth cycles of the electrodes with spines made from the three alloys discussed above are shown in Fig. 8(a) - (c). The capacity of electrodes with alloy spines ( $d = 4.15 \text{ g cm}^{-3}$ ) is greater than

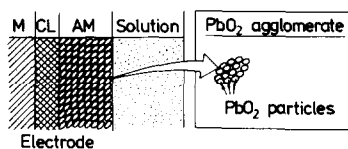


Fig. 7. Models of  $PbO_2$  powder electrode and  $PbO_2$  agglomerate.

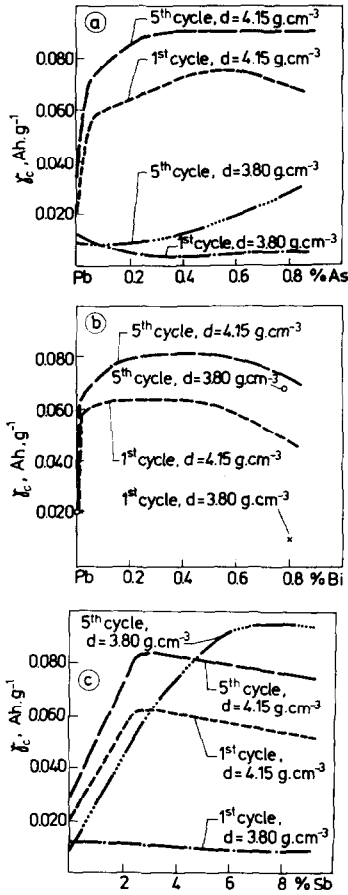


Fig. 8. Comparison of capacity/alloy-additive curves for first and fifth cycle for electrodes with (a) Pb-As, (b) Pb-Bi, (c) Pb-Sb spines.

that of electrodes using lead. This capacity enhancement could be due to the following two reasons.

(i) Arsenic, bismuth and antimony ions can lower the value of the combined polarization  $\Delta\phi_{CL/AM} + \Delta\phi_{Agg} + \Delta\phi_{Pi}$  and can thus increase the number of the agglomerates that participate in the discharge process. This may be caused by the inclusion of the dopant ions in the interfaces of the agglomerates. For the same type of polarizations, Fig. 3 shows that when arsenic and antimony ions are present in the electrolyte, the ions reduce the capacity of the powder electrodes with a lead spine. Under the same conditions, bismuth ions result in a capacity increase. The influence of dopant ions depends on the mode by which the ions are introduced into the electrode system.

(ii) During the spine corrosion, arsenic, antimony, and bismuth alloy components are oxidized and included in the corrosion layer composition.

The polarizations  $\Delta\phi_{M/CL} + \Delta\phi_{CL} + \Delta\phi_{CL/AM}$  can decrease under the dopants' influence. The latter can result from the incorporation of the dopant ions in the crystal lattice of the  $PbO_2$  particles in the corrosion layer, thus causing a conductivity increase and/or highly conductive Pb-dopant oxides to be formed. This action of arsenic, bismuth, and antimony reduces the role of the corrosion layers as a capacity-limiting factor and increases the possibilities of active-mass utilization.

On the first discharge, the values of  $\Delta\phi_{CL/AM} + \Delta\phi_{Agg}$  are quite high for many agglomerates so they do not take part in the discharge process. All electrodes have a low initial capacity. The capacity is determined by those parts of the agglomerates that have electronic contact between them, as well as with the corrosion layer. Comparison of the capacities at the first and the fifth cycles from Fig. 8 shows that:

$$(\Delta\phi_{CL/AM} + \Delta\phi_{Agg}) = f(d, D) \quad (4)$$

At a density  $d = 3.80 \text{ g cm}^{-3}$ , all electrodes yield lower capacities on the first cycle than those with a Pb spine. After five cycles, however, the capacity values of the alloy-spine electrodes are much higher than those of electrodes with a Pb spine. Apparently, arsenic, antimony, and bismuth stimulate the processes of structure restoration. Antimony exhibits the strongest influence, bismuth a weaker one, while arsenic displays the least pronounced influence of the three dopants.

Capacity curves for Pb-As, Pb-Bi, and Pb-Sb spine electrodes at the 20th cycle are shown in Fig. 9. It can be assumed that the active-mass skeleton structure is already formed at the 20th cycle. The data reveal that the dopants act with different efficiencies on the restoration processes of the active-mass structure. For example, for electrodes with a powder density of  $4.15 \text{ g cm}^{-3}$ , a 50% active-mass utilization is achieved with alloy component concentrations of 0.2 wt.% Bi (=0.2 at.% Bi) and 0.86 wt.% As (=2.34 at.% As) for Pb-Bi and Pb-As spines, respectively. By contrast,

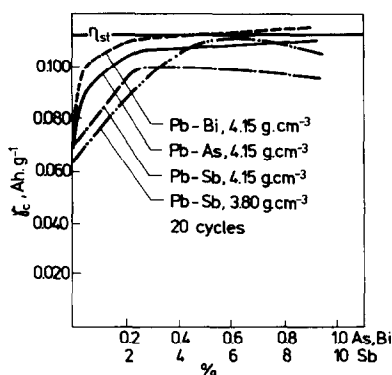


Fig. 9. Comparison of capacity/alloy-additive curves for 20th cycle for electrodes with (a) Pb-As, (b) Pb-Bi, (c) Pb-Sb spines.

6 wt.% Sb (=9.8 at.% Sb) is required for electrodes using Pb-Sb spines and having a powder density of  $3.80 \text{ g cm}^{-3}$ . It is clear, therefore, that Pb-Sb spines demand a high alloy component concentration but exert a beneficial effect at lower active-mass density.

Figures 6 and 9 show that the capacity curves of the Pb-Sb electrodes pass through a maximum at the 20th cycle. For electrodes with  $d = 3.80 \text{ g cm}^{-3}$ ,  $\gamma_{c, \max}$  is observed with a Pb-6wt.%Sb spine, while for electrodes with  $d = 4.15 \text{ g cm}^{-3}$  the capacity maximum is obtained with a Pb-2.3wt.%Sb spine. This may be due to the formation of some mixed lead-antimony oxides. At a higher density (smaller pore volume), a lower antimony content is required for such oxide formation.

A comparison of Fig. 6(a) and (b) reveals a very important experimental finding. At the 20th cycle, the capacity of electrodes with  $d = 3.80 \text{ g cm}^{-3}$  is higher than that for electrodes with  $d = 4.15 \text{ g cm}^{-3}$ , despite the fact that the density of the discharge current is higher for the former electrodes. Figure 4 shows that the situation is reversed when Pb-As spines are used, while Fig. 5 demonstrates that the capacities at both active-mass densities are approximately equal when Pb-Bi spines are employed. It is clear, therefore, that the differences in electrode capacity are not caused by hindrances to the ion transport in the active mass. More probably, the dopants change the nature of the  $\text{PbO}_2$  particles in the active mass.

In all the studies of the powder electrode reported here, it has been assumed that polarizations due to the electrochemical reaction, and ion-transport hindrance in the pores, are both quite small and remain unchanged with the introduction of the dopants. This assumption may not be valid for the electrochemical reaction.

In conclusion, the investigations discussed here have shown that the tubular electrode is a convenient construction for examining the action of dopants on the component elements of the positive lead/acid battery plate, and their interconnection and development into the active-mass structure.

## References

- 1 I. K. Gibson, K. Peters and F. Wilson, in J. Thomson (ed.), *Power Sources 8*, Academic Press, London, 1980, p. 565.
- 2 F. Arifuku, H. Yoneyama and H. Tamura, *J. Appl. Electrochem.*, 9 (1979) 629, 635.
- 3 D. Barrett, M. T. Frost, J. A. Hamilton, K. Harris, I. R. Harrowfield, J. F. Moresby and D. A. J. Rand, *J. Electroanal. Chem.*, 118 (1981) 131.
- 4 B. K. Mahato, *J. Electrochem. Soc.*, 126 (1979) 365.
- 5 H. N. Cong, A. Ejjenne, J. Brenet and P. Faber, *J. Appl. Electrochem.*, 11 (1981) 373.
- 6 D. E. Sweets, *J. Electrochem. Soc.*, 120 (1973) 925.
- 7 A. Arifuku, H. Yoneyama and H. Tamura, *J. Appl. Electrochem.*, 11 (1981) 357.
- 8 E. J. Ritchie and J. Burbank, *J. Electrochem. Soc.*, 117 (1970) 299.
- 9 J. L. Dawson, M. I. Gillibrand and J. Wilkinson, in D. H. Collins (ed.), *Power Sources 3*, Oriol Press, Newcastle upon Tyne, 1970, p. 1.
- 10 W. Hermann and G. Propstl, *Z. Elektrochem.*, 61 (1957) 1154.
- 11 A. A. Abdul Azim and A. A. Ismail, *J. Appl. Electrochem.*, 7 (1977) 119.

- 12 T. Rogachev, G. Papazov and D. Pavlov, *J. Power Sources*, 10 (1983) 291.
- 13 S. Felin and M. Morcillo, *Corros. Sci.*, 15 (1975) 593.
- 14 J. Burbank, *J. Electrochem. Soc.*, 118 (1971) 525.
- 15 N. A. Hampson, S. Kelly and K. Peters, *J. Appl. Electrochem.*, 10 (1980) 91, 261.
- 16 A. Boggio, M. Maja and N. Penazzi, *J. Power Sources*, 9 (1983) 221.
- 17 I. H. Yeo and D. C. Johnson, *J. Electrochem. Soc.*, 134 (1987) 1973.
- 18 D. Pavlov, E. Bashtavelova, V. Manev and A. Nassalevska, *J. Power Sources*, 19 (1987) 15.
- 19 D. Pavlov, in L. J. Pearce (ed.), *Power Sources 11*, Pergamon Press, London, 1987, p. 165.
- 20 D. Pavlov and T. Rogachev, *Power Sources*, Praha Zari, Dum Techniky CVTS, Praha, CSSR, 1975, p. 53.
- 21 D. Pavlov and E. Bashtavelova, *J. Electrochem. Soc.*, 133 (1986) 241.
- 22 D. Pavlov and E. Bashtavelova, *J. Electrochem. Soc.*, 131 (1984) 1468.